Archives of Microbiology (2023) 205:277
https://doi.org/10.1007/s00203-023-03608-7

ORIGINAL PAPER

Deposition of *Daldinia starbaeckii* (ELF) functionalized silver nanoparticles on urinary catheter tube using chitosan polymer to prevent microbial biofilms formation during UTI infection

Shweta Bharti[1,2] · Balwant Singh Paliya[3] · Sanjeeva Nayaka[1] · Rajesh Kumar[2]

Received: 9 February 2023 / Revised: 25 May 2023 / Accepted: 9 June 2023 / Published online: 7 July 2023

Abstract

Catheter-associated urinary tract infections (CAUTI) are the most common healthcare problem in hospitals. In this study, we isolated the *Daldinia starbaeckii* (An endolichenic fungus from *Roccella montagnie*) and its biomass extract were used to simultaneously synthesize and deposit DSFAgNPs on the inner and outer surfaces of the catheter tube using chitosan biopolymer via In-situ deposition method. Perfectly designed *D. starbaeckii* extract functionalized DSFAgNPs were characterized by UV spectroscopy, FTIR, SEM, EDS, TEM, and XRD. The microbial efficacy of DSFAgNPs & DSFAgNPs coated catheter (CTH3) was evaluated against eight human pathogenic gram (+/−) ive strains and *Candida albicans*. Results indicated DSFAgNPs showed significant biological activity against both gram (+/−) ive bacteria with an average MIC_{90} of 4 µl/ml. The most promising activity was observed against *Helicobacter pylori*. When bacteria strains allow to grow with CTH3 we reported significant reduction in colony formation unit (CFU/ml) in broth culture assay with an average 70% inhibition. Further, antibiofilm activity of CTH3 against *P. aeruginosa* showed strong inhibition of biofilm formation (85%). The study explored an alternate approach for significantly prevent CAUTI among hospital patients.

Graphical abstract

We isolated an endolichenic fungus from lichen *Roccella montagnei*. The molecular characterization of fungus identified as *Daldinia starbaeckii* (DSF). The DSF was cultured and its fungal biomass exudes were used to simultaneously construct DSF-AgNPs and its deposition on the catheter surface using biopolymer chitosan via In-situ deposition method. Further, antimicrobial and antibiofilm efficacy of DSF-AgNPs was checked against urinary catheter contaminating and human pathogenic

Communicated by Gharieb El-Sayyad.

✉ Rajesh Kumar
rajesh4971@yahoo.com

Shweta Bharti
shweta.scmat@gmail.com

[1] Lichenology Laboratory, CSIR-National Botanical Research Institute, Lucknow 226001, India

[2] Department of Microbiology, Babasaheb Bhimrao Ambedkar Central University, Lucknow 226025, India

[3] Department of Biotechnology, Bundelkhand University, Jhansi 284128, India

bacterial strains. Based on our research, we determined that DSF-AgNPs coating on a urinary catheter through this method is a cost-effective, eco-friendly approach to prevent catheter contamination.

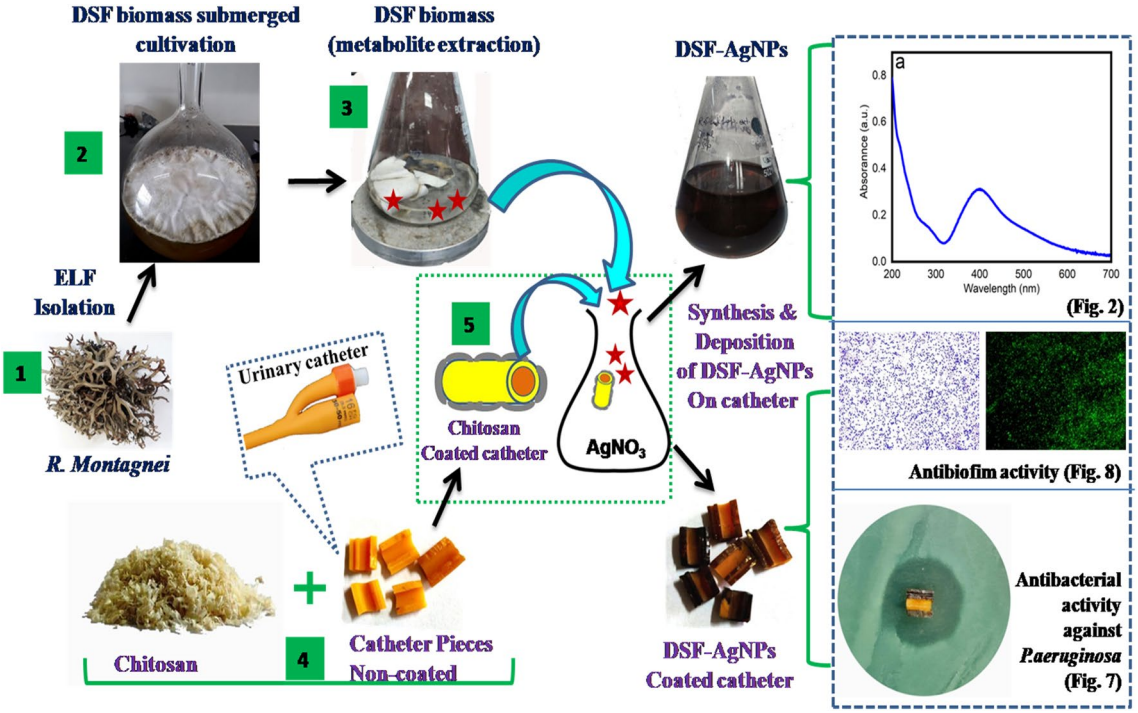

Keywords Antimicrobial · Endolichenicfungus · Greennanotechnology · Lichen · *Roccella montagnie*

Abbreviations

EDAX	Energy Dispersive X-ray Analysis
CAUTI	Catheter-associated urinary tract infections
ELF	Endolichenic fungus
DSF	*Daldinia starbaeckii* Fungus
MIC	Minimum inhibitory concentration
CFU	Colony forming unit
RT	Room temperature
NPs	Nanoparticles
ZOP	Zone of Prohibition
QS	Quorum sensing
rpm	Rotation per minute

Introduction

The advances in the medical field exclusively rely on the ever-increasing use of various biomedical devices, frequently required in the treatment/diagnosis of chronic and acquired diseases of people. Urethral catheters are the most widely used biomedical device installed to manage the drain urethra of the patient temporarily both in hospitals and other care units. It is estimated that more than 100 million urinary catheters are marketed every year and 61% of catheters are categorically used among intensive care unit (ICUs) patients (Bhatia et al. 2010; Greene et al. 2014; Saint et al. 2000; Trautner and Darouiche 2004; Weinstein et al. 1999). Despite many desirable properties of these biomaterials like mechanical strength, ease of mold, and biocompatibility, the catheter's surface is prone to getting contaminated by bacterial colonization. Therefore, patients are susceptible to Catheters associated urinary tube infections (CAUTI). It was reported that 50% of patients develop an infection when catheters are used for 7–10 days with a 3–6% risk added up with each day. The major cause of catheter contamination is the formation of biofilms (A threshold population of pathogenic bacteria produced layers of exopolysaccharides polymeric matrix over the bacterial colony) by pathogenic microbe on the surface of indwelling catheters. Biofilms protect bacteria against the host immune system and antibiotics and provide favorable conditions for further flourishing. To prevent or minimize catheter contaminations through microbial biofilms formation several ongoing efforts have been made such as modification of catheters surface by antibiofilm and bactericidal agents. However, many pathogenic bacteria developed drug resistance to these conventional antibiotics and shifted the need for alternate antimicrobial agents (Lo et al. 2014; Schumm and Lam 2008).

The continued discovery of new pathogenic microorganisms created a challenge for researchers and the medical field. Therefore in the last few decades, the majority of researchers shifted their attention to nanotechnology. In this field, green nanotechnology has been used to synthesize metal nanoparticles (silver, zinc, gold, etc.) using biological agents. The method is cost-effective, eco-friendly, and non-toxic and particles synthesized using this technique showed remarkable bioactive properties that may be for a multifunctional human welfare approach (Gupta et al. 2018; Ranjani et al. 2021).

In the search for unique bioactive phytomolecules, most of the researchers draw their attention to lower groups of plants and fungus such as lichens. Lichens are a marvelous group of the fungi kingdom and are naturally assembled by the consortium of fungi and algae (Honegger 2009). Lichens are endowed with unique bioactive metabolites and have been used as important traditional medicine in many cultures. However, in nature, lichens have diverse umpteen microorganisms (endolichenic fungus) that help to make lichen's unique bioactive metabolites. Endolichenic fungus (ELF) (endosymbionts) is defined as the diverse array of fungal communities that exist intracellularly in the host lichen thallus, they associate with lichen photobiont for their nutrition, without causing any deleterious symptoms. ELF is quite different from lichenicolous fungus. ELF has an ecological group that is distinct from endophytic fungi. ELF is an ocean of a hidden source of novel bioactive compounds. Silver ions of $AgNO_3$ brilliantly decorate and incorporate the ELF bioactive compounds through physicochemical reduction (Behera et al. 2006; Stocker-Wörgötter 2001; Stocker-Wörgötter and Elix 2004).

The study aims to focus on the isolation of ELF from *Roccella montagnei* lichen and its identification. One of the pure cultures, ELF was identified as *Daldinia starbaeckii* fungus (DSF). Then biomass culture extract of DSF was used to simultaneously synthesize silver nanoparticles (DSF-AgNPs) and their deposition on the inner and outer surface of the urinary catheter tube using a chitosan biopolymer layer. *R. montagnei* contains varieties of unique secondary metabolites and has been significantly used for its pharmaceutical properties such as antimicrobial, anti-inflammatory, and larvicidal activities (Anjali et al. 2014; Balaji et al. 2006) Therefore, synthesized nanoparticles were evaluated for antimicrobial activity against human pathogens, including strains causing catheter-associated urinary tract infection (CAUTI). Best of my knowledge, there are no previous reports of silver nanoparticle synthesis using endolichenic fungus *Daldinia starbaeckii* from lichens.

Materials and methods

The lichen (*Roccella montagnei*) was collected from konark, Odisha, India and authenticated by Dr. Sanjeeva nayaka (senior principle scientist, lichenology department, CSIR-NBRI, Lucknow, India). Silver nitrate (Sigma Aldrich), Antibiotic disc (HiMedia) for positive control, Catheter tube (Foley catheter, silicon coated latex catheter Fr 16, 5.3 mm) purchase from local medical shop of Lucknow, India.

Isolation of endolichenic fungus (ELF) and its culture

First, the *Roccella montagnei* was gently clean with a soft brush under running water (3 times) to eliminate the unwanted particles; again the sample was washed through tween 80 and was washed through running water unless detergents were completely removed. Subsequently, the lichen sample was washed with Mili-Q water and kept for drying on blotting paper for two days at room temperature (RT) to completely dry.

The dry lichen samples were dissected and transferred onto PDA (potato dextrose agar) Petri plates; incubate for 3 to 7 days at 25 ± 2 °C. When the hyphal tips emerged out from lichen segments they were isolated, subculture, and brought to pure culture by serial sub-culturing. Pure fresh grown ELF was inoculated in fresh PDB (Potato dextrose broth) media and incubated for 10 to 15 days at 25 ± 2 °C and the culture was checked for contamination at regular intervals. When sufficient ELF biomass was grown, the media was removed and biomass was washed with double distilled water. For metabolite extraction ELF biomass was boiled in 100 ml mili-Q water at 75 °C for one hour and Whatman No. 42 filter paper (pore size 2.5 µm) was used to filter it. Finally, the filtrate was kept at 4 °C for further experimental research work.

Molecular identification of ELF

Pure fungal mycelia were harvested and transferred onto fresh PDA slants and Identified by 18S rRNA gene amplification and sequencing by CSIR-NCCS, Pune. The phylogenetic tree was constructed with the help of MEGA-X (Molecular Evolution Genetic Analysis) software. "BLAST search" (https://blast.ncbi.nlm.nih.gov/Blast.cgi) was used to compare the maximum similarity of nucleotide sequences (consensus sequences) and recognition of correct ELF species (Azuddin et al. 2021; Rahaman et al. 2020).

Biological synthesis of DSF-AgNPs and surface modification of urinary catheter

The surface modification of the catheter by DSF-AgNPs was carried out on a latex Foley catheter, silicone coated (Fr 16,

5.3 mm) were purchased from the local medical shop in Lucknow, India. The catheter was chopped into small pieces (CTH1) and further cut laterally to expose the inner surface too. Then catheter pieces were sequentially washed with mili Q and 70% ethanol and dried completely at RT, before being kept in air-tight packets for a future experiment.

The DSF-AgNPs deposition process is performed in two steps. First, sterilized catheter pieces were incubated in 1% chitosan solution (in 1% v/v acetic acid) for 24 h on a stirrer at 200 rpm. Then catheter pieces were taken out, rinsed with distilled water, and dry in a hot air oven at 40 °C for 1 h. Subsequently, 100 ml of 0.1 mM $AgNO_3$ solution was taken in a 250 ml flask and chitosan-coated catheter pieces (CTH2) were added to the solution. The mixture was kept on a magnetic stirrer at 200 rpm maintaining the temperature of 60 ℃. To this solution DSF filtrate was added drop-wise, adjusting the solution to approx. pH 8 using 1 M NaOH. Synthesis of DSF-AgNPs and simultaneous deposition of DSF-AgNPs on chitosan-coated catheter was analyzed by observing a change in color of the solution, and the final surface modified catheter (CTH3) into brown.

Instruments used for characterization of DSF-AgNPs

Preliminary characterization of the DSF-AgNPs was monitored by measuring absorption spectra between 200 and 700 nm wavelength using a UV spectrophotometer, Then, DSF-AgNPs solution was centrifuged at 12,000 rpm for 20 min. and the pellet was washed with Milli Q water. This process was repeated three times and the final pellet was dried at room temperature. Further FTIR spectrum analysis of DSF-AgNPs was done using instrument Model: Nicole 6700, Make Thermo-Scientific, USA. All the measurements were carried out in the range of 400–4000 cm^{-1} at a resolution of 4 cm^{-1}. Scanning electron microscopy (SEM) analysis was performed by FEI Quanta 250 (FEI, The Netherlands) at a working accelerating voltage of 30 kV to determine the morphology and shape of DSF-AgNPs. EDAX technique was used for elemental analysis of DSF-AgNPs using SEM Instrument. While, Transmission electron microscopy (TEM, JEOL JEM 1400 Tokyo, Japan, operating at accelerating voltage 40–120 keV) was done to evaluate the size distribution of DSF-AgNPs. For TEM analysis samples were prepared by drops coating on the copper TEM grid and left for air dry. After solvent evaporation, DSF-AgNPs get embedded on-grid and examined under TEM (Gade et al. 2008). Phase identification of the DSF-AgNPs was done using X-ray diffractometry (XRD), Model: D8 Advance Eco, Make: Bruker, Germany. Average hydrodynamic size distribution and Zeta-potential (mV) of DSF-AgNPs was determined using Anton-Paar, Litesizer™ 500, USA Zetasizer.

Screening of biological activity

Antimicrobial activity and minimum inhibitory concentration assay of DSF-AgNPs

To determine the broad spectrum antimicrobial efficacy of DSF-AgNPs including CAUTI associated pathogens the synthesized nanoparticles were checked for antimicrobial activity against 9 pathogenic strains (*H. pylori, S. mutans, S. aureus, E. coli, P. aeruginosa, S. typhimurium, K.pnemoniae, A. baumannii, and Candida albicans*) using standard disc diffusion assay (Laupland et al. 2005). Overnight grown microbes culture in Luria broth was centrifuged at 5000 rmp for 10 min and pellets were reconstitute in 0.85% NaCl solution to prepare Standard cell solution (SCS) by adjusting cell concentration to 0.5 at OD_{600} nm. 100 µl of freshly prepared SCS of Microbial pathogens was uniformly spread on agar plates using a sterile spreader and left on the plates at 30 °C for approximately 30 min. The seeded Petri plates were used for the saturation of the distinct concentrations of DSF-AgNPs suspension (1, 2, 3 & 4 µg/ml) onto the filter paper discs, 20 µl on each disc and incubated at 37 ± 2 °C overnight. Subsequently, DSF-AgNPs created a zone of prohibition against the microbial pathogen around the disc, which was measured in mm units by finding the growth of the pathogens cells disappearance around the paper discs. For MIC_{90} (for 90% growth inhibition) value determination, Alamar blue assay was performed in 96 well cell culture plates according to company product guideline protocol. (https://www.gbiosciences.com/image/pdfs/protocol/786-921_protocol.pdf).

Antibacterial activity of DSF-AgNPs coated urinary catheter

Subsequently, the antibacterial activity of CTH1, CTH2, and CTH3 was determined through colony forming unit (CFU/ml) on agar plate assay. Briefly, the fresh culture of all bacterial strains was prepared in Nutrient broth and incubated for 24 h at 37 °C. 200 µl of broth culture (cell density 3×10^5/ml) was mixed with 1.8 ml of sterile artificial urine (pH 7.4), prepared according to the standard protocol described earlier, and placed in 6 well cell culture plates (Din et al. 1999). Then different catheter samples (CTH1, CTH2 and CTH3) were put into the mixture in separate wells and plates kept in a shaker incubator for 24 h, 37 °C, and 100 rpm. Afterward, catheter pieces were removed and gently washed with 1X PBS twice to remove planktonic cells. The bacteria adhering to the catheter surface was resuspended into 1X PBS solution and shaken vigorously on vortex, after removing catheter pieces, 10 µl of this mixture was spread on NA agar plates evenly and incubated the plates for 24 h at 37 °C. Results were recorded by counting Colony forming units CFU on agar plates.

Further, explored the antibacterial activity of modified catheters against two prominent catheter contaminating bacteria *P. aeruginosa* and *E.coli* were determined through agar disc diffusion assay by replacing the disc with catheter samples.

Antibiofilm activity

The Antibiofilm property of synthesized DSF-AgNPs was evaluated before coating it on urinary catheter tubes against *P. aeruginosa* according to the method given by Paliya et al. 2021 with some modifications. Bacterial biofilms was allowed to grow on glass slides in 6 well cell culture plates for 24 h supplemented with different concentrations (0.5, 1 & 1.5 µg/ml) of nanoconjugates sample. After biofilms formation on glass slides, it will wash with 1X Phosphate buffer saline and stained with crystal violet. Stained biofilms will be observed under a microscope for evaluation. To investigate the antibiofilm effect on the surface-modified catheter (CTH3), *P. aeruginosa* GFP (ATCC® 15692GFP™) strain was allowed to grow overnight in the nutrient broth. The CTH3 was incubated with 2 ml of bacterial broth culture ($OD_{600} = 0.01$). Then biofilms were allowed to grow statically for 24 h. Biofilm formed on CTH3 tube was transferred on UV sterilized polycarbonate filter membrane and then on glass slides followed by fixing with 70% isopropanol and dried by heating in hot air oven at 40 °C. The biofilms are washed with 1X PBS to remove any planktonic cells and inhibition will determine under a fluorescence microscope (Leica, Germany) at 40× magnification (Paliya et al. 2021). Further, quantitative estimation of biofilms production due to bacterial load on formed biofilm was determined by resuspending crystal violet stained biofilms (taken from the previously performed test) in 0.5 ml ethanol (95%) for five minutes and OD of dissolved crystal violet was measured at 650 nm (Imperi et al. 2013).

Statistical analysis

All the experiments were performed in n number of biological replicates. The results of experiments were calculated as mean ± SD (where, $n = 3$) and data significant at $p = 0.05$. MIC_{90} results represented as ≤ or ≥ to treated concentration.

Results and discussion

Phylogenetic analysis of ELF

Endolichenic isolate of *Roccella montagnei* was identified through the internal transcribed spacer (ITS) nucleotide-based sequences method. According to BLAST results, the isolated strain was identified as *Daldinia starbaeckii,* maximum symmetry was expressed by phylogenetic tree nearly 99% with the antecedently *Daldinia starbaeckii* strain. *Daldinia* species belong to the phylum Ascomycota. The constructed phylogenetic tree of *Daldinia* species depicted in (Fig. 1) comes in line with the prior morphologically, identified *Daldinia* strain (Mostert et al. 2014). The Gen Bank accession number of the present endolichenic fungal (*Daldinia starbaeckii)* strain was OM095441.

Synthesis and deposition of DSF-AgNPs on the catheter surface

To enhance the stability of the coating agent over the catheter surface we choose biopolymer chitosan. Initially, the chitosan layer was embedded on the catheter surface followed by ELF extract merged on the chitosan-coated catheter surface. The significance of this step is explained as chitosan and extract, both are the biological agent and there should be a high possibility of natural bonding between them through different functional groups. Further, the present approach allows the direct synthesis of DSFAgNPs in solution and NPs deposition over catheter surface, rather than coating NPs through extra steps, using various costly techniques. A systematic diagram in the graphical abstract showed the

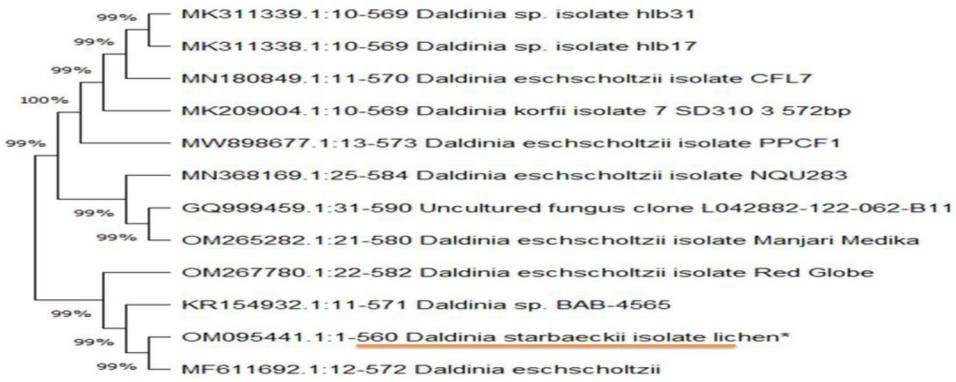

Fig. 1 Phylogenetic analysis of *D. starbaeckii* (NCBI accession no. OM095441) with closely related sequences retrieve from NCBI Genbank

whole process of catheter coating with DSF-AgNPs. Primary confirmation of DSF-AgNPs deposition over catheter surfaces was a change in color of catheter surface from dark pale yellow to dark brown. This occurs due to surface plasmon resonance (SPR) phenomena i.e., plasmon oscillation at the same frequency corresponds to the light electric field and is a characteristic phenomenon that appears during phase transition (in this particular case transition of Ag^+ ion into DSF-AgNPs (Chen and Ming 2012).

Characterization of DSFAgNPs

UV–Vis spectroscopic analysis showed a sharp characteristic peak of DSF-AgNPs in the range of 400–420 nm (Fig. 2a and b). The DSF biomass excreted proteins and metabolites in solution were served for Ag^+ ions fictionalization and stabilization. The energy required by an electron to achieve the highest occupied electron orbital from the lowest unoccupied orbital known as the optical energy band gap (Eg) of the DSF-AgNPs was calculated by 'Tauc's plot' ($Eg = hc/\lambda$ (eV) (Fig. 2a). The estimated Eg value of the DSF-AgNPs is ~2.5 eV. The band gap energy of AgNPs was lower than in prior published articles and this lower value of optical band gap might be due to endolichenic fungus secondary components that cover the nanoparticles surface and was not conflict with quantum confinement effect (Barzinjy and Azeez 2020; Maheshwaran et al. 2020). FTIR spectroscopy graph gives the idea about the capping and interactions of bimolecular with silver ions which is responsible for stabilization of DSF-AgNPs. IR spectrum is very complex because of the overlap of frequencies in the same region (Fig. 3a). However, we have attempted to identify the involvement of biomolecules through shifts in stretching vibrations after the formation of DSF-AgNPs. IR spectrum of DSF-AgNPs and ELF extract demonstrated functional group stretch vibration peaks correspond to each other with small deviation representing involvement of those particular groups in nanoparticles synthesis. The stretched vibration at peaks ranging 3433–3445 cm^{-1} represents the absorption stretch of primary amine NH. A peak at 2165.7 cm^{-1} in the DSF-AgNPs graph represents the thiocyanate group (–SCN). Thiocyanate is a strong oxidizing agent (Chandler and Day 2012). A peak in the range of 1680–1620 cm^{-1} showed the alkenyl group, C = C stretch. The next peak at 1550–1650 cm^{-1} represents aliphatic nitro compound or secondary amine, NH bend. Other peaks at 1409.8, and 652.3 cm^{-1} correspond to the presence of vinyl C-H in-plane bend, alkyne C = H bends (John 2006). This concludes that all functional groups change stretching frequencies and excellently reduce the $AgNO_3$ to AgNPs. These all functional groups act as strong capping agents of AgNPs and are also involved in stabilization.

SEM micrographs of DSF-AgNPs were taken without coating and after coating on the catheter, SEM images revealed rough spherical morphology of NPs with a size range of 20–100 nm (Fig. 4a–c). Particles seem to be got embedded in the chitosan layer which could be a possible reason for the stable coating of NPs. Similarly. TEM images also confirmed that DSF-AgNPs were nearly spherical and polydispersed with a size range of 10–50 nm (Fig. 4d). Further, EDAX elemental analysis showed an Ag peak indicating particle composition AgNPs (Fig. 5a). The DLS analysis showed the hydrodynamic size of NPs, represented in particle size distribution histogram. The average hydrodynamic

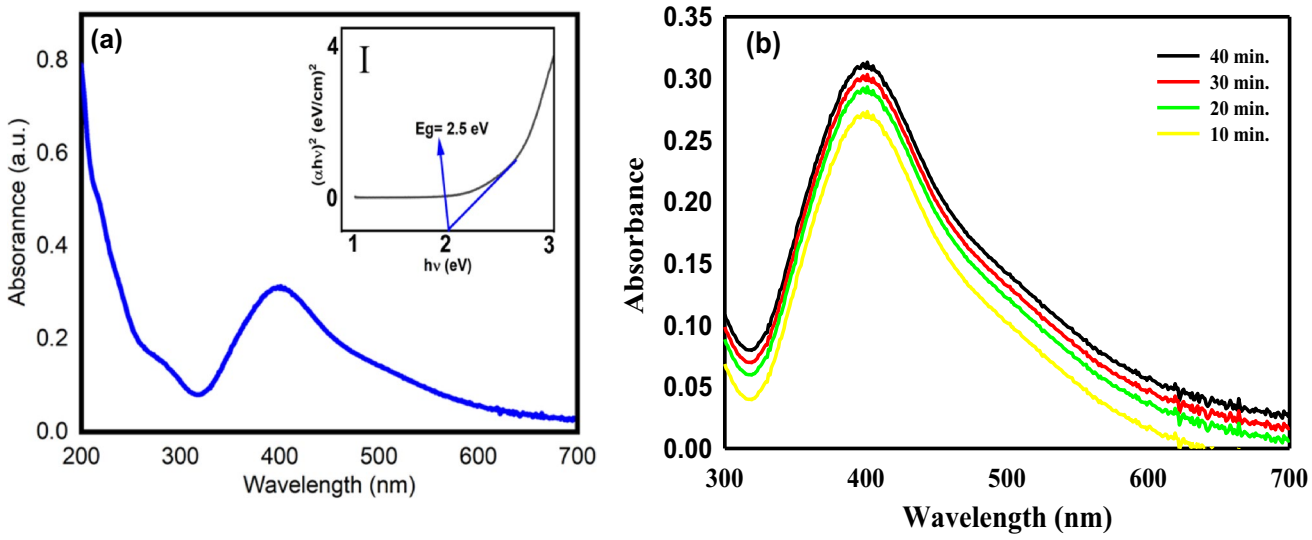

Fig. 2 **a** Absorbance spectrum with inset of Tauc's plot. **b** UV-Spectrophotometer absorbance graph represented characteristic absorption peaks at wavelength 400–420 nm in different time intervals

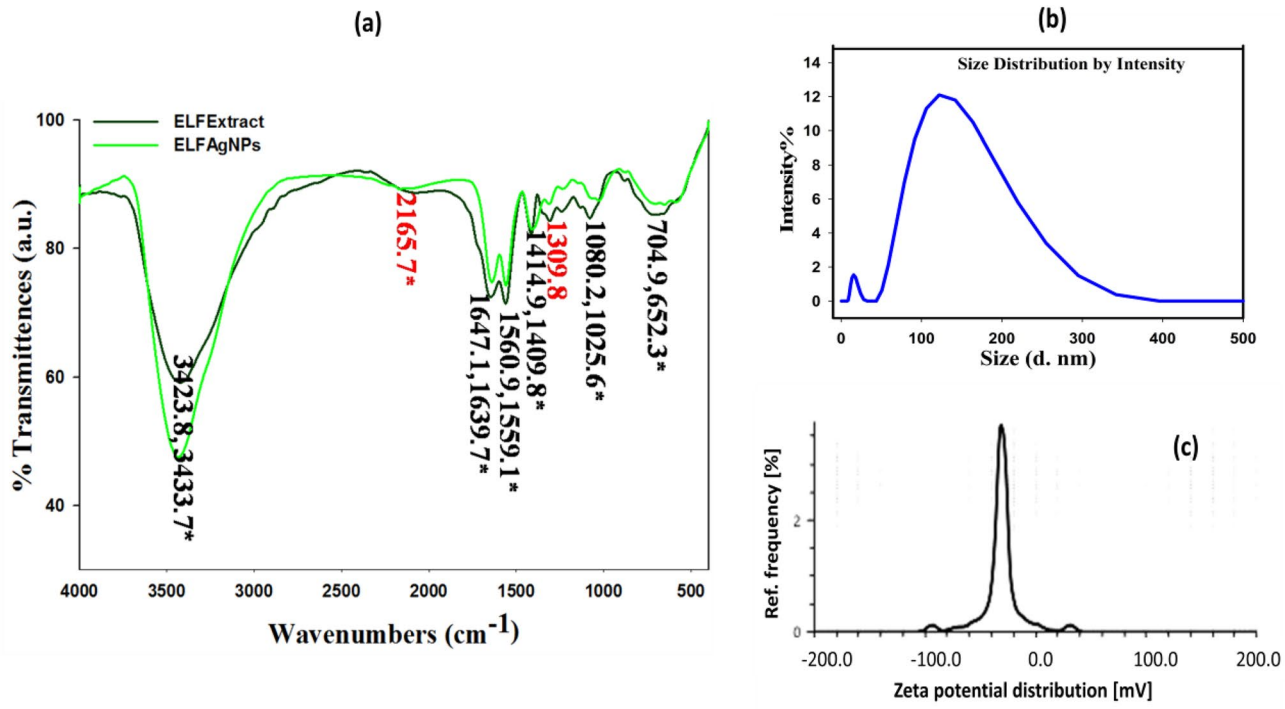

Fig. 3 **a** FTIR spectra of *D. starbaeckii* extract and DSF-AgNPs before and after bioreduction. **b** DLS graph, showed size distribution of synthesized NPs. **c** Zeta-potential analysis of DSF-AgNPs

diameter size and zeta-potential value of DSF-AgNPs were 120 ± 10 nm and − 30 mV (Fig. 3c). The increased diameter size of synthesized NPs could be due to less-polar DSF- phytomolecules encapsulation on NPs or agglomeration due to hydrophobic interaction between particles. The particles are synthesized at 60 °C and dried at 70–80 °C before using in experiments. So we suggested that particles thermally stable upto 80 °C.

X-ray diffraction graph showed intense peaks at 2θ angles of 37.747, 45.992, 64.200, 77.070, and 81.268 which is corresponding to the planes (111), (200), (202), (311) (222) respectively (Fig. 5c). XRD pattern indicating the unit cell structure of DSF-AgNPs is face-centered cubic (fcc) according to (JCPDS File No. 04–0783) with a lattice parameter of $a = 4.077$ Å. Few more intense diffraction peaks at 2θ angles of 43.992°, 54.602°, and 57.097°, 85.509 might be related to Ag_2O. Secondary metabolites are found in the ELF that is oxygenated. It would have been embraced during the synthesis of ELF-AgNPs (Cheng et al. 2018).

Biological activity

Antimicrobial activity of DSF-AgNPs

The synthesized DSFAgNPs exhibited plausible biological activity, corresponding to change in concentrations, against all screened pathogenic microorganisms. The most significant activity was observed at a maximum concentration of 4 µg/ml. Results were presented as Zone of prohibition (ZOP). *A. baumannii* (19 ± 0.58), *C. albicans* (16.3 ± 0.57), *E. coli* (18.67 ± 1.15), *H. pylori* (23 ± 2.3), *K. pneumoniae* (16.67 ± 1.5), *P. aeruginosa* (18.6 ± 0.5), *S. aureus* (14.3 ± 0.97), *S. mutans* (17.8 ± 1.6), *S. tiphimurium* (19.8 ± 2.2) (Fig. 6a). Among all pathogens, excellent growth suppression by DSFAgNPs was observed against *H. pylori*, zone of prohibition (ZOP) 23 ± 0.5 mm as compared to positive control streptomycin ZOP. The MIC value demonstrated the viability of pathogens after their exposure to DSFAgNPs. The DSFAgNPs efficiently inhibited *P. aeruginosa* which was represented by MIC viability test 4 µg/ml, ZOP 18.6 ± 0.5, and *H. pylori* 2 µg/ml. MIC value of the remaining strain was represented in Fig. 6b and Table 1. Previously reported *Daldinia* species (*D. eschscholtzii*) exhibited good activity against *Bacillus subtilus, Candida albicans*, *Escherichia coli*, and *Staphylococcus aureus* (Katoch et al. 2017; Kandou et al. 2021). In biological screening, we observed that the DSFAgNPs showed notable activity against gram-negative microorganisms as compared to gram-positive microorganisms *S. aureus* ZOP 14.3 ± 0.5 with MIC value 12 µg/ml. Several other studies showing antimicrobial effect of green synthesized silver nanoparticles using different lichens extracts (Alavi et al. 2019; Alqahtani et al. 2020).

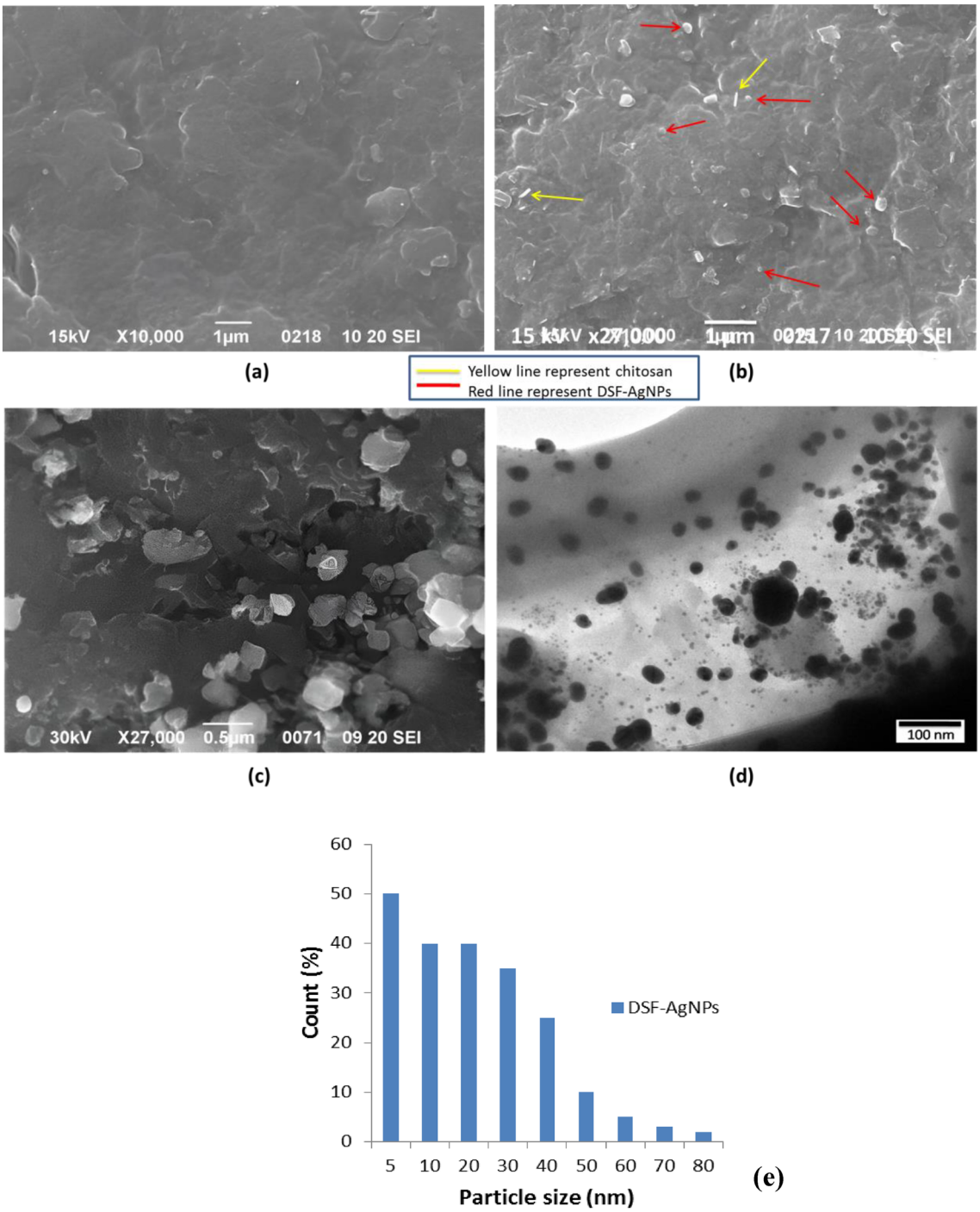

Fig. 4 Represent SEM & TEM image **a** catheter surface image without any surface modification **b** catheter surface modified by chitosan and DSF-AgNPs coating. Image showed embedded chitosan fibers and DSF-AgNPs over catheter surface. **c** SEM image of DSF-AgNPs. **d** and **e** TEM image of DSF-AgNPs and Particle size distribution (nm)

Antimicrobial activity of DSF-AgNPs coated urinary catheter

Results clearly indicated (Fig. 7a) that CTH3 exhibit strong antibacterial activity against *P. aeruginosa* and *E. coli*. However, no special action was observed in CTH2 and CTH1. ZOP of CTH3 was 17 ± 0.56 mm against *P. aeruginosa* and 19 ± 0.67 mm against *E. coli*. Similarly, colony-forming assay results were analyzed by counting single colonies formed on agar plates. The CFU counts of the

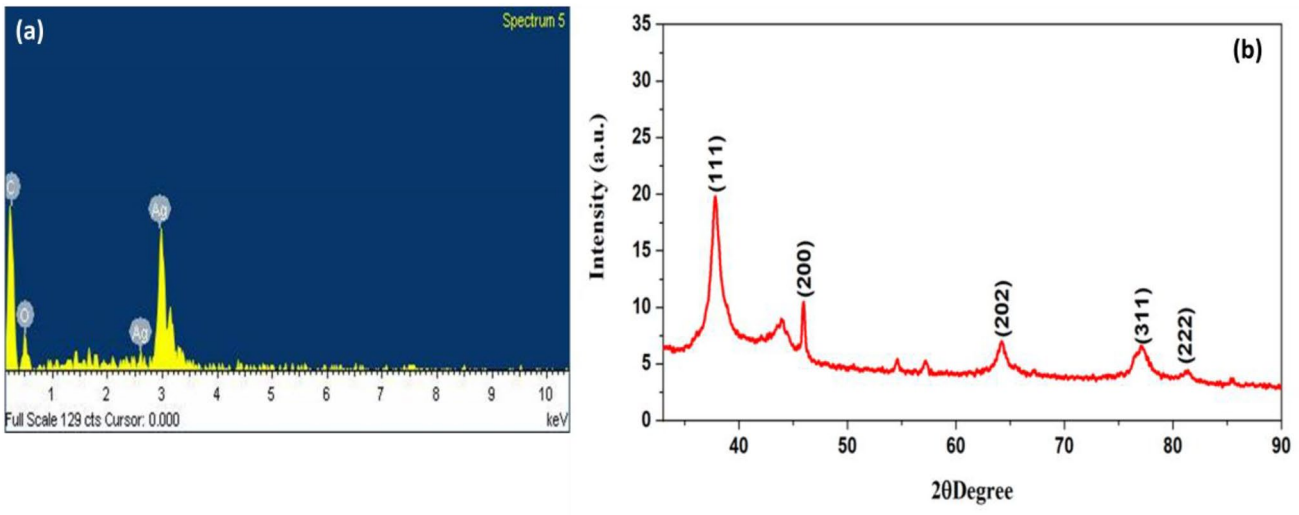

Fig. 5 **a** EDAX, elementary analysis of synthesized NPs. **b** X-ray diffraction showed DSF-AgNPs crystal lattice diffraction peaks at 2θ angle

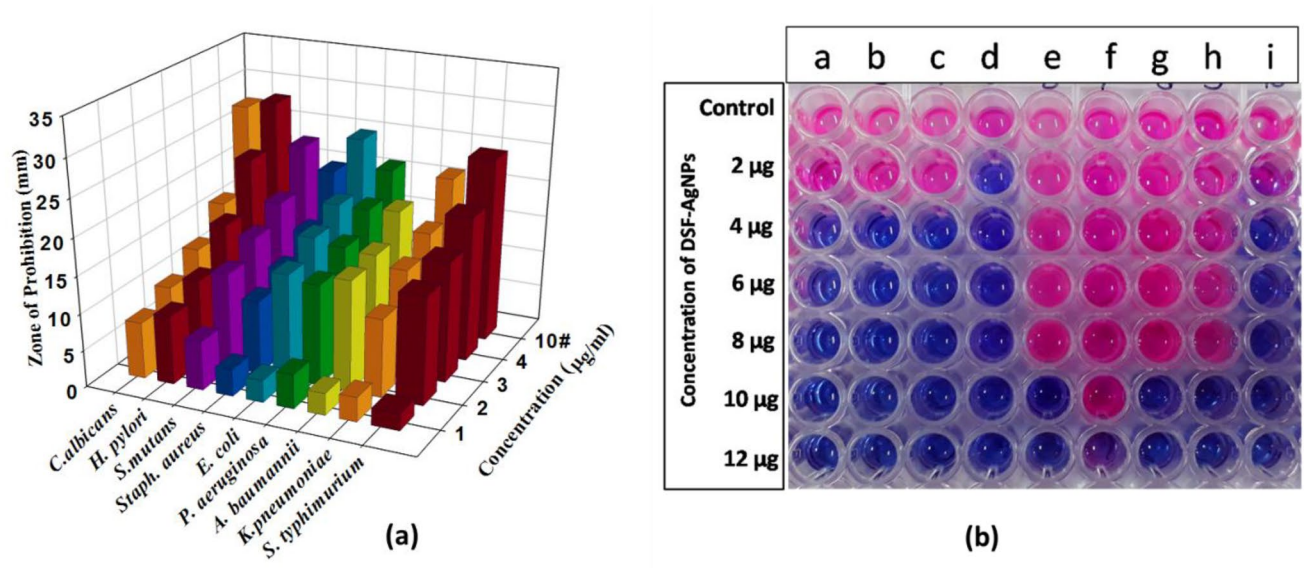

Fig. 6 **a** Antimicrobial activity of DSF-AgNPs on agar disc diffusion assay. **b** Minimum inhibitory concentration value of DSF-AgNPs against human pathogenic microbial strains

Table 1 Minimum Inhibitory Concentration (MIC) of DSFAgNP against tested micobes in µg/ml

Microbial strains	*S. typhimurium* (a)	*S. mutans* (b)	*P. aeruginosa* (c)	*H. pylori* (d)	*E. coli* (e)	*Staph. aureus* (f)	*A. baumannii* (g)	*K. pneumoniae* (h)	*C. albicans* (i)
MIC value (µg/ml)	≤4	≤4	≤4	≤2	≤10	>12	≤10	≤10	≤4

CTH3-treated plate were significantly less than those compared to CTH2 and CTH1 was indicated that DSF-AgNPs can also release from the coated surface in a fluid environment (Fig. 7b). This further demonstrated the effectiveness of DSF-AgNPs coated catheters (CTH3) during indwelled urinary drainage conditions.

Biofabricated AgNPs execute antimicrobial action by adhering to the bacterial membrane. This adhesion of

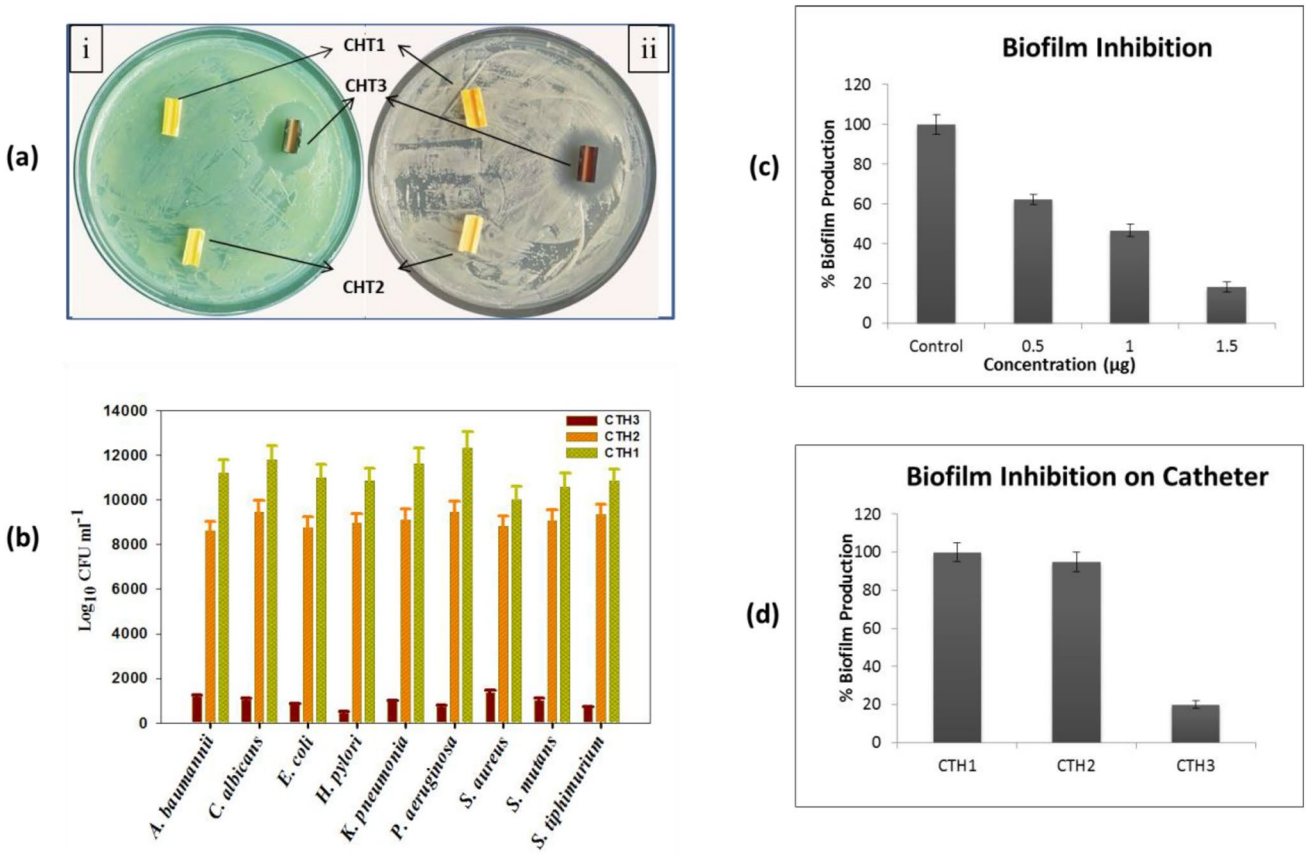

Fig. 7 **a** Microbial zone of prohibition on agar plates (i) *P. aeruginosa* and (ii) *E.coli*. **b** Graph represent numbers of colony forming units after 24 h treatment by DSF-AgNPs coated catheter and data was represented as $\log_{10}$ CFU ml^{-1} ($2 \times 10.^{3}$). **c** Percent biofilm production in DSF-AgNPs treated test samples. **d** Percent biofilm production on catheters. Data were represented as mean of three independent experiments. Whereas, error showed standard deviation. Data significant at $p = 0.05$

AgNPs on the bacterial cell was favored by the charge on AgNPs which was dependent on the strategy of the method of synthesis. DSF-AgNPs showed a small negative charge (− 11 mV) thereby favoring its attachment to bacterial cells (Gordon et al. 2010). The possible mechanism of DSF-AgNPs antibacterial activity is an internalization of NPs into the cell or by attaching to the cell surface outside. In both, cases DSF-AgNPs disrupt the membrane potential and damage the cell wall and cell membrane leading to cell content leakage. Damage cells allow more DSF-AgNPs internalization causing dysfunction of lipids, proteins, and DNA synthesis. AgNPs have been reported to generate a high concentration of reactive oxygen species (ROS) which get interact with important enzymes and eventually stop bacterial growth (Losasso 2014).

Antibiofilm forming effect

The critical problem faced while using catheters is contamination by bacterial biofilm formations. In the following experiment, antibiofilm property of CTH1, CTH2 and CTH3 was determined against the most common medical device contaminating bacteria *P. aeruginosa*. This strain has an evolutionary benefit of biofilms formation and can able to form biofilms on biotic and abiotic surfaces as well. Biofilms of *P. aeruginosa* are highly resistant to antimicrobial drugs, therefore conventional drugs and methods are not as effective against it. The results showed a percentage of biofilms production in the Invitro experiment treated with DSF-AgNPs (0.5, 1 & 1.5 µg/ml) was 62 ± 2.8. 46.7 ± 3.0 and 18.2 ± 2.5 (Fig. 7c). Moreover, biofilm production on CTH1, CTH2, and CTH3 catheters is shown in (Fig. 7d). Microscopic analysis showed that biofilm formed in DSF-AgNPs treatments was distorted, uneven, and thin with less amount of exopolysaccharides secretion. Whereas, the biofilms layer formed over CTH2 and CTH1 are thick and continuous with a significant number of bacterial cell embedded bacterial indicating that DSF-AgNPs is a potential antibiofilm agent (Fig. 8a and b). Interestingly, things to be noticed is that DSF-AgNPs can significantly inhibit biofilms formation on catheters under invitro condition which predominantly contains many

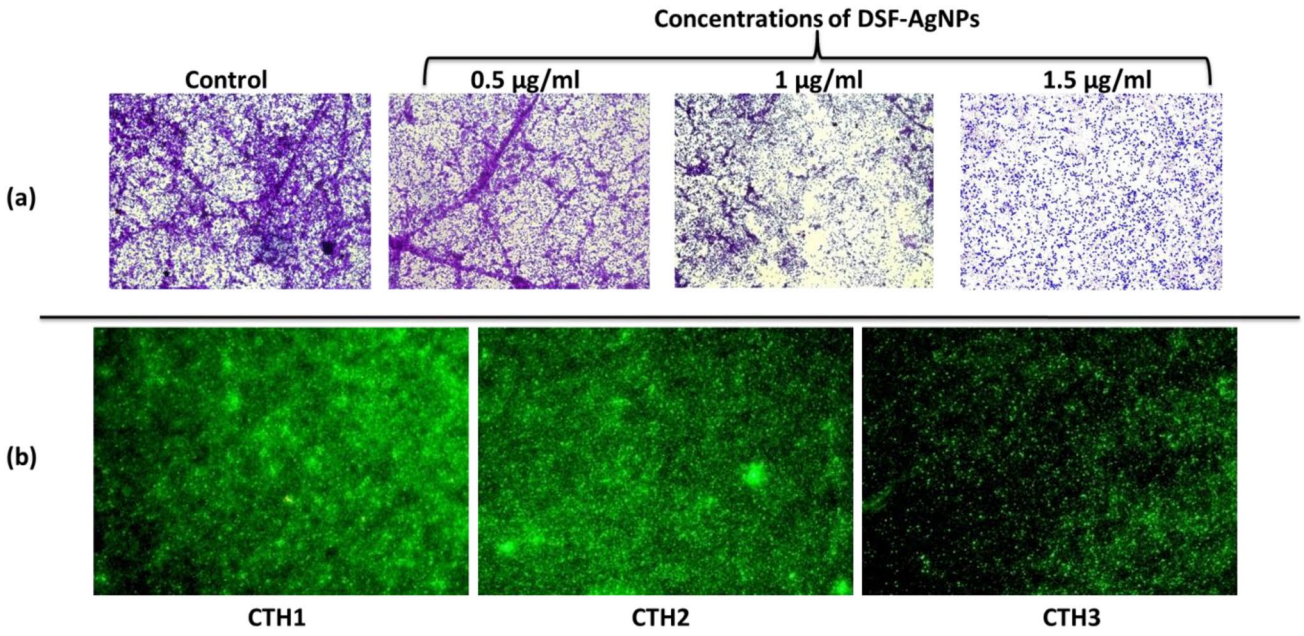

Fig. 8 Effect of DSF-AgNPs on biofilm formation against *P. aeruginosa* strains. **a** Inhibition of biofilm formation in DSF-AgNPs treated PA01. **b** Inhibition of biofilm formation on coated surface or non-coated surface catheters against *P. aeruginosa* GFP

bacteria inoculums compared to the natural condition of urethra indwelling.

The possible mechanism underlying the antibiofilm activity of DSF-AgNPs was inhibition of bacterial protein synthesis and enzyme productions. Since biofilms production in *P. aeruginosa* is regulated through quorum sensing (QS) gene regulation and virulence factors productions. Also, the QS mechanism is triggered at a certain threshold population density, whereas the growth inhibitory effect of DSF-AgNPs further limits bacteria to form biofilms (Losasso et al. 2014).

Conclusion

Nature has its own way of synthesizing unique chemical substances, a prime example of which is lichens. And lichens give the researchers unique endolichenic fungus. We explore the endolichenic fungus (*Daldinia starbaeckii*) uniqueness in our research work and conclude that DSF-AgNPs-coated catheters can successfully inhibit bacterial growth and biofilms formation over catheters surfaces. Using biopolymer chitosan for deposition of nanoparticles over catheters surface is the cheapest and most harmless method for catheters surface modification with antimicrobial agents and could replace market available costly catheters prepared using complex multi steps methods. Since AgNPs exhibits different mode of action for antimicrobial activity, therefore, present modification of catheters will work against different microbial strains including drug-resistant bacteria and probably be a better solution for CAUTI. Moreover, using endolichenic fungus can make it possible to utilize unique bioactive metabolites of lichens without harming their ecological status. However, few evaluations regarding DSF-AgNPs toxicity to human skin (urethra) need to be done before any In-vivo trials.

Acknowledgements The authors are thankful to the Director, CSIR-National Botanical Research Institute, Lucknow for providing laboratory facilities and the Vice Chancellor, BBAU, Lucknow for providing research-oriented environment. The author is also grateful to Prof. Rajesh Kumar, my supervisor/mentor, who always helped and encouraged me to achieve any research goals.

Author contributions Shweta Bharti: Conceptualization, Investigation, Writing - Original Draft, Data Curation, Formal analysis, B.S. Paliya: Writing - Review & Editing, Visualization. Sanjeeva Nayka: Supervision Validation, Review & Editing Rajesh Kumar: Supervision, Conceptualization, Editing.

Funding This research did not receive any specific grant from funding agencies in the public, commercial, or not-for-profit sectors.

Data availability The sequence data generated during the current study of Daldinia starbaeckii are available in the Genbank repository under accession numbers OM095441.

Declarations

Conflict of interest The authors declare that they have no conflict of interest.

References

Alavi M et al (2019) Antibacterial, antibiofilm, antiquorum sensing, antimotility, and antioxidant activities of green fabricated Ag, Cu, TiO_2, ZnO, and Fe_3O_4 NPs via *Protoparmeliopsismuralis* lichen aqueous extract against multi-drug-resistant bacteria. ACS Biomater Sci Engine 5:4228–4243

Alqahtani M et al (2020) Biofabrication of silver nanoparticles with antibacterial and cytotoxic abilities using lichens. Sci Rep 10:16781

Anjali DB et al (2014) Antimicrobial activity of lichen *Roccella montagnei* Bél. obtained from Horsley hills, Andhra Pradesh, India. In: Madhusudhana Rao J (ed) Bioactives from natural products. Proceedings of Andhra Pradesh Academy of Sciences. p 13–20

Azuddin NF et al (2021) Molecular phylogeny of endophytic fungi from rattan (*Calamus castaneus* Griff.) spines and their antagonistic activities against plant pathogenic fungi. J Fungi 7:301

Balaji P et al (2006) In vitro antimicrobial activity of *Roccella montagnei* thallus extracts. J Trop Med Plant 7:169–173

Barzinjy AA, Azeez HH (2020) Green synthesis and characterization of zinc oxide nanoparticles using *Eucalyptus globulus* Labill. leaf extract and zinc nitrate hexahydrate salt. SN Appl Sci 2:991

Behera BC, Adawadkar B et al (2006) Tissue-culture of selected species of the Graphis lichen and their biological activities. Fitoterapia 77:208–215

Bhatia N et al (2010) Urinary catheterization in medical wards. J Glob Infect Dis 2:83–90

Chandler JD, Day BJ (2012) Thiocyanate: a potentially useful therapeutic agent with host defense and antioxidant properties. Biochem Pharmacol 84:1381–1387. https://doi.org/10.1016/j.bcp.2012.07.029

Chen Y, Ming H (2012) Review of surface plasmon resonance and localized surface plasmon resonance sensor. Photonic Sens 2:37–49

Cheng L et al (2018) Potential antibacterial mechanism of silver nanoparticles and the optimization of orthopedic implants by advanced modification technologies. Int J Nanomed 13:3311

Din EN 1616:1999. (1999) Sterile urethral catheters for single use; german institute for standardisation (Deutsches Institut für Normung). Berlin, Germany, p 1–16

Gade AK et al (2008) Exploitation of *Aspergillus niger* for synthesis of silver nanoparticles. J Biobased Mater Bioenergy 2:243–247

Gordon O et al (2010) Silver coordination polymers for prevention of implant infection: thiol interaction, impact on respiratory chain enzymes, and hydroxyl radical induction. Antimicrob Agents Chemother 54:4208–4218

Greene MT et al (2014) Regional variation in urinary catheter use and catheter-associated urinary tract infection: results from a national collaborative. Infect Control Hosp Epidemiol 35:S99-106

Gupta N et al (2018) Applications of silver nanoparticles in plant protection. Springer, Cham, pp 247–265

Honegger R (2009) Lichen-forming fungi and their photobionts. In: Plant relationships. Springer, Berlin, Heidelberg, p 307–333

Imperi F et al (2013) New life for an old drug: the anthelmintic drug niclosamide inhibits *Pseudomonas aeruginosa* quorum sensing. Antimicrob Agents Chemother 57:996–1005

John Coates (2006) Interpretation of infrared spectra, a practical approach. Encyclopedia of Analytical Chemistry. John Wiley & Sons Ltd

Kandou FE et al (2021) Molecular identification and antibacterial activity of marine-endophytic fungi isolated from sea fan *Annella* sp. from Bunaken waters, Manado, North Sulawesi, Indonesia. Aquac Aquar Conserv Legis 14:317–327

Katoch M et al (2017) Phylogeny, antimicrobial, antioxidant and enzyme-producing potential of fungal endophytes found in *Viola odorata*. Ann Microbiol 67:529–540

Laupland KB, Bagshaw SM, Gregson DB, Kirkpatrick AW, Ross T, Church DL (2005) Intensive care unit-acquired urinary tract infections in a regional critical care system. Crit Care 9:R60-65

Lo E et al (2014) Strategies to prevent catheter-associated urinary tract infections in acute care hospitals: 2014 update. Infect Control Hosp Epidemiol 35:464–479

Losasso C (2014) Antibacterial activity of silver nanoparticles: sensitivity of different *Salmonella serovars*. Front Microbiol 5:227

Maheshwaran G et al (2020) Green synthesis of Silver oxide nanoparticles using *Zephyranthes Rosea* flower extract and evaluation of biological activities. J Environ Chem Eng 8:104137

Mostert L et al (2014) Taxonomy and pathology of Togninia (Diaporthales) and its Phaeoacremonium anamorphs. Stud Mycol 77:1–43

Paliya BS et al (2021) Evaluation of anti-quorum sensing potential of *Saraca asoca* (family Caesalpiniaceae) against *Chromobacterium violaceum* and *Pseudomonas aeruginosa* PA01. J Pharm Res Int 33:71–82

Rahaman MS et al (2020) Molecular phylogenetics and biological potential of fungal endophytes from plants of the Sundarbans Mangrove. Front Microbiol 11:570855

Ranjani S et al (2021) Synthesis, characterization and applications of endophytic fungal nanoparticles. Inorg Nano-Met Chem 51:280–287

Saint S et al (2000) Are physicians aware of which of their patients have indwelling urinary catheters? Am J Med 109:476–480

Schumm K, Lam TB (2008) Types of urethral catheters for management of short-term voiding problems in hospitalized adults: a short version Cochrane review. Neurourol Urodyn 27:738–746

Stocker-Wörgötter E (2001) Experimental lichenology and microbiology of lichens: culture experiments, secondary chemistry of cultured mycobionts, resynthesis, and thallus morphogenesis. Bryol 104:576–581

Stocker-Wörgötter E, Elix JA (2004) Experimental studies of lichenized fungi: formation of rare depsides and dibenzofurans by the cultured mycobiont of *Bunodophoron patagonicum* (Sphaerophoraceae, lichenized Ascomycota). Bibl Lichenologica 88:659–669

Trautner BW, Darouiche RO (2004) Catheter-associated infections: pathogenesis affects prevention. Arch Intern Med 164:842–850

Weinstein JW et al (1999) A decade of prevalence surveys in a tertiary-care center: trends in nosocomial infection rates, device utilization, and patient acuity. Infect Control Hosp Epidemiol 20:543–548